

INFLUENCE OF QUANTUM CONFINEMENT ON THE HEAT CAPACITY
OF GRAPHITE

KAMAKHYA P. GHATAK and SAMBHU N. BISWAS

*Department of Electronic Science, University of Calcutta, 92 Acharya Prafulla
Chandra Road, University College of Science and Technology, Calcutta-700009,
India*

and

*Department of Electronics and Telecommunication Engineering, Bengal
Engineering College, Shibpur, Howrah - 711103, West Bengal, India*

Received 15 March 1993

UDC 538.95

PACS 65.40.Em

In this paper an attempt is made to investigate theoretically the heat capacity in graphite having quantum confinement in one, two and three dimensions such as quantum wells, quantum wires, quantum dots and magneto-sized quantization of band states. The appropriate density of states functions are deduced, taking into account various types of anisotropies of the energy band constants. It has been found that the heat capacity oscillates with the film thickness, magnetic film and doping in various manners. The heat capacity is largest in quantum dots and smallest in quantum wells. The theoretical analysis is in agreement with the experimental results.

1. Introduction

In recent years, with the advent of fine lithographical methods [1], molecular beam epitaxy [2], organometallic vapour-phase epitaxy [3] and other experimental techniques, low-dimensional structures [4-6], having quantum confinement in one, two and three dimensions (such as quantum wells, quantum wires, quantum dots and magneto-sized quantization), have attracted much attention not only for their potential in uncovering new phenomena in thermal analysis, but also for their various device applications. In quantum wells (QWs), due to the presence of the quantum size effect, the electrons are confined in 2D films [2]. In quantum wells wires (QWWs), the two directions of motions are quantized and electrons can only propagate in a single direction [8]. In quantum dots (QDs), the wave-vector space is totally quantized and the 3D quantization occurs [9]. The 3D quantization can also occur under magneto-sized quantization (MSQ) since in the presence of a quantizing magnetic field, the density of states becomes the Dirac delta function in QWs due to the influence of Landau quantization [10]. Although many new effects associated with quantum confinements have already been reported, there still remain topics for investigation as the interest for further research on different other aspects of various thermal compounds is becoming increasingly important. One such important property is the heat capacity (HC) of such materials. The HC of the carriers in different metals and semiconductors have been reported under various physical conditions [11-14]. Nevertheless, it appears that the HC in quantum confined graphite has yet to be investigated under the aforementioned quantization of band states by considering the anisotropies of the energy band constants. Besides, since the Mott insulators and the microelectronic devices are usually being distinguished by the characteristic of HC, and the speed of operation of the thermal quantum confined devices is directly proportional to it, it would be of much interest to investigate the heat capacity in quantum confined graphite, particularly at low temperature where the aforementioned quantum effects become important and also when the phonon contribution to such capacity becomes negligible. We shall investigate the HC in QWs, QWWs, QDs and MSQs of graphite. We shall study the doping, magnetic field and film thickness dependence of HC in such graphite microstructures.

2. Theoretical background

A. Formulation of HC in QWs of graphite

The total heat capacity can be written [15] as

$$C = C_1 + C_2. \quad (1)$$

C_1 is the lattice heat capacity. For the present case it can be expressed as [15]

$$C_1 = (4k_B T / \theta_D^2) \int_0^{\theta_D/T} y^3 \exp(-y) [1 - \exp(-y)]^{-2} dy \quad (2)$$

where k_B is the Boltzmann constant, T is the temperature and θ_D is the Debye temperature. C_2 is the electronic heat capacity which can, in turn, be expressed as [16]

$$C_2 = \int EN(E) \left[\frac{E - E_F}{T} + \frac{dE_F}{dT} \right] \frac{df_o}{dE} dE, \quad (3)$$

where $N(E)$ is the density of states function, E_F is the Fermi energy, f_o is the Fermi-Dirac occupation probability factor and E is the total energy of the carriers. The term (dE_F/dT) can be obtained from the expression of carrier concentration ($n_o = \int N(E)f(E)dE$) by substituting $(dn_o/dT) = 0$, since at low temperatures, where such quantum confined devices operate and the quantum effects become prominent, such substitution becomes justified on physical grounds [18].

It appears that the formulation of the HC in the present case requires expressions of $N(E)$ and n_o which are determined by the appropriate electron energy spectrum. The $E - \mathbf{k}$ dispersion relation of the conduction electrons in graphite can be written [17,21] as

$$E = \frac{1}{2}[E_2 + E_3] \pm \left[\frac{1}{4}(E_2 - E_3)^2 + \eta_2^2 k^2 \right]^{1/2}, \quad (4)$$

where

$$E_2 = [\Delta - 2\gamma_1 \cos \phi + 2\gamma_5 \cos^2 \phi],$$

$$\phi = ck_z/2$$

$$k^2 = k_x^2 + k_y^2 + k_z^2$$

$$E_3 = 2\gamma_2 \cos^2 \phi$$

$$\eta_2 = (\sqrt{3}/2)a(\gamma_o + 2\gamma_4 \cos \phi).$$

where the physical meaning of the band parameters have been defined in Ref. 17.

Therefore, the electron energy spectrum in QWs of graphite can be expressed as

$$c(n)k_s^2 = [E - A(n)]^2 - B(n) - C(n)(n\pi/d_z)^2, \quad (5)$$

where

$$A(n) = \frac{1}{2}[\Delta - 2\gamma_1 \cos(Cn\pi/2d_z) + 2\gamma_5 \cos^2(Cn\pi/2d_z) + 2\gamma_2 \cos^2(Cn\pi/2d_z)].$$

$n = 1, 2, \dots$ is the size quantum number along the z -direction,

$$B(n) = \frac{1}{4}[\Delta - 2\gamma_2 \cos(Cn\pi/2d_z) + 2\gamma_5 \cos^2(Cn\pi/2d_z) - 2\gamma_2 \cos^2(Cn\pi/2d_z)]^2$$

$$C(n) = (2a^2/4)[\gamma_0 + 2\gamma_4 \cos(Cn\pi/2d_z)]^2,$$

$$k_s^2 = k_x^2 + k_z^2$$

and d_z is the film thickness along the z direction. The use of Eq. (5) leads to the expression for the density of states function as

$$N(E) = (2\pi)^{-1} \sum_{n=1}^{n_{max}} [E - A(n)]\Theta(E - E_n)/C(n) \quad (6a)$$

where Θ is the Heaviside step function and E_n can be determined from the equation

$$E_n = A(n) \pm [B(n) + C(n)(n\pi/d_z)^2]^{1/2}. \quad (6b)$$

Thus, combining Eq. (5) with the Fermi-Dirac occupation probability factor, the surface electron concentration can be expressed as

$$n_o = (k_B T/2\pi) \sum_{n=1}^{n_{max}} C^{-1}(n)[k_B T F_1(\eta) + F_o(\eta)\{E_n - A(n)\}], \quad (6c)$$

where $\eta = (k_B T)^{-1}(E_F - E_n)$, E_F is the Fermi energy and $F_j(\eta)$ is the one-parameter Fermi-Dirac integral of order j [18,19]. The use of Eq. (6c) leads to the expression of E'_F (the prime denotes the differentiation with respect to T) as

$$E'_F = [p_1(n)p_2^{-1}(n)], \quad (7)$$

where

$$\begin{aligned} p_1(n) = & [-n_o/T + (k_B T/2\pi) \sum_{n=1}^{n_{max}} C^{-2}(n)C'(n)[k_B T F_1(\eta) + F_o(\eta)\{E_n - A(n)\} - \\ & -(k_B T/2\pi) \sum_{n=1}^{n_{max}} C^{-1}(n)[k_B T F_{-1}(\eta) - k_B F_o(\eta)\eta - F_o(\eta)E'_n + \\ & F_o(\eta)\{E'_n - A'(n)\}] + F_{-1}(\eta)\{-(\eta/T) - (E'_n/k_B T)(E_n - A(n))\}] \end{aligned}$$

and

$$p_2(n) = [(k_B T/2\pi) \sum_{n=1}^{n_{max}} C^{-1}(n)[F_o(\eta) + F_{-1}(\eta)(k_B T)^{-1}(E_F - A(n))]].$$

Combining Eqs. (3), (6a) and (7) we get

$$C_2 = \sum_{n=1}^{n_{max}} [f_1(E_F) + f_2(E_F)](2\pi)^{-1}, \quad (8)$$

where

$$f_1(E_F) = \left\{ (E/C(n))[E - A(n)] \left[\frac{E - E_F}{T} + \frac{p_1(n)}{p_2(n)} \right] \right\}_{E=E_F}$$

$$f_2(E_F) = \sum_{r=1}^S q_r [f_1(E_F)].$$

r is the set of real positive integers,

$$q_r = 2(k_B T)^{2r} (1 - 2^{1-2r}) \zeta(2r) \frac{d^{2r}}{dE_F^{2r}},$$

and $\zeta(2r)$ is the zeta function of order $2r$ [20].

3. Formulation of HC in QWW of graphite

Eq. (5) leads to the expression for the electron dispersion law in QWWs of graphite as

$$C(n)k_x^2 = [E - A(n)^2] - B(n) - C(n)(n\pi/d_z)^2 - C(n)(t\pi/d_y)^2, \quad (9)$$

from which follows

$$k_x^2 = (E^2/C(n)) + \overline{C}_1(n) - \overline{C}_2(n)E, \quad (10)$$

where

$$\overline{C}_1(n) = C^{-1}(n)[A^2(n) - B(n) - C(n)\pi^2\{n^2d_z^{-2} + t^2d_y^{-2}\}].$$

t and d_y are the size quantum number and the thickness, respectively, and $\overline{C}_2(n) = 2A(n)/C(n)$. Therefore, the density of states function is given by

$$N(E) = \frac{1}{4\pi} \sum_{n=1}^{n_{max}} \sum_{t=1}^{t_{max}} C_3(E, n) \Theta(E - E_4(n)) \quad (11)$$

where

$$C_3(E, n) = [2EC^{-1}(n) - \overline{C}_2(n)] \left[\frac{E^2}{C(n)} + \overline{C}_1(n) - \overline{C}_2(n)E \right]^{-1/2}$$

and $E_4(n)$ is obtained by putting $E = E_4(n)$ and $k_x = 0$ in Eq. (10). The use of Eq. (11) leads to the expression of electron concentration per unit length in QWWs of graphite as

$$n_o = (2\pi)^{-1} \sum_{n=1}^{n_{max}} \sum_{t=1}^{t_{max}} [f_3(E_F, n) + f_4(E_F, n)], \quad (12)$$

where

$$f_3(E_F, n) = [E_F^2 - C^{-1}(n) + \overline{C}_1(n) - E_F \overline{C}_1(n)]^{1/2},$$

E_F is the Fermi energy in the present case and

$$f_4(E_F, n) = \sum_{r=1}^S q_r [f_3(E_F, n)].$$

Using Eq. (3) the electronic heat capacity for QWW of graphite can be expressed as

$$C_2 = (4\pi)^{-1} \sum_{n=1}^{n_{max}} \sum_{t=1}^{t_{max}} [f_5(E_F, n) + f_6(E_F, n)], \quad (13)$$

where

$$f_5(E_F, n) = \left[EC_3(E, n) \left[\frac{E - E_F}{T} + \frac{dE_F}{dT} \right] \right]_{E=E_F}$$

and

$$f_6(E_F, n) = \sum_{r=1}^S q_r [f_5(E_F, n)],$$

where $\frac{dE_F}{dT}$ can be obtained from Eq. (12) by putting $\frac{dn_o}{dT} = 0$.

4. Formulation of HC in QDs of graphite

Following Eq. (10), the modified electron dispersion law for QDs of graphite can be written as

$$(\pi u/d_x)^2 = (E^2/C(n)) + \overline{C}_1(n) - \overline{C}_2(n)E, \quad (14)$$

where u and d_x are the size quantum number and the thickness along the x -direction, respectively. Eq. (14) leads to the expression for the density of states function as

$$N(E) = \frac{1}{d_o d_y d_z} \sum_{n=1}^{n_{max}} \sum_{t=1}^{t_{max}} \sum_{u=1}^{u_{max}} \delta'(E - E_5), \quad d_o = d_x/2, \quad (15)$$

where δ' is the Dirac delta function and E_5 is obtained from Eq. (14) by putting $E = E_5$. Thus, the electron concentration can be expressed as

$$n_o = \frac{1}{d_o d_y d_z} \sum_{n=1}^{n_{max}} \sum_{t=1}^{t_{max}} \sum_{u=1}^{u_{max}} F_{-1}(\eta_1), \quad (16)$$

where $\eta_1 = (k_B T)^{-1}(E_F - E_5)$ and E_F is the Fermi energy. From Eq. (16) we can write

$$Z_1 = \left[\sum_{n=1}^{n_{max}} \sum_{t=1}^{t_{max}} \sum_{u=1}^{u_{max}} F_{-2}(\eta_1) \right]^{-1} \left[\sum_{n=1}^{n_{max}} \sum_{t=1}^{t_{max}} \sum_{u=1}^{u_{max}} (k_B \eta_1 + E_5') F_{-2}(\eta_1) \right]. \quad (17)$$

In this case C_2 is given by

$$C_2 = (d_o d_y d_z k_B T)^{-1} \sum_{n=1}^{n_{max}} \sum_{t=1}^{t_{max}} \sum_{u=1}^{u_{max}} E_5 \{ T^{-1}(E_F - E_5) - Z_1 \} \times \\ \times \exp\left(\frac{E_5 - E_F}{k_B T}\right) \left[1 + \exp\left(\frac{E_5 - E_F}{k_B T}\right) \right]^{-2}. \quad (18)$$

5. The HC in graphite under magneto-sized quantization

The electron dispersion law assumes the form

$$2c(n) \left[\frac{2eH}{2\hbar} \left(w + \frac{1}{2} \right) \right] = [E - A(n)]^2 - B(n) - C(n)(n\pi/d_z)^2, \quad (19)$$

where H is the quantizing magnetic field along z -direction and w is the Landau quantum number. The density of states function can be written as

$$N(E) = \frac{2eH}{h} \sum_{n=1}^{n_{max}} \sum_{w=0}^{w_{max}} \delta'(E - E_6), \quad (20)$$

where E_6 is obtained from Eq. (19) by putting $E = E_6$. The electron concentration can be expressed as

$$n_o = \frac{2eH}{h} \sum_{n=1}^{n_{max}} \sum_{w=0}^{w_{max}} F_{-1}(\eta_2) \quad (21)$$

where

$$\eta_2 = (E_F - E_6)(k_B T)^{-1}$$

and E_F is the Fermi energy. Eq. (21) leads to the expression $dE_F/dT = Z_2$, where

$$Z_2 = \left[\sum_{n=1}^{n_{max}} \sum_{w=0}^{w_{max}} F_{-2}(\eta_2) \right]^{-1} \left[\sum_{n=1}^{n_{max}} \sum_{w=0}^{w_{max}} (k_B \eta_2 + E'_6) F_{-2}(\eta_2) \right].$$

In this case C_2 is given by

$$C_2 = \frac{2eH}{hk_B T} \sum_{n=1}^{n_{max}} \sum_{w=0}^{w_{max}} E_6 T^{-1} (E_F - E_6) - Z_2 \exp\left(\frac{E_6 - E_F}{k_B T}\right) \left[1 + \exp\left(\frac{E_6 - E_F}{k_B T}\right) \right]^{-2}. \quad (22)$$

6. Results and discussion

Using Eqs. (1) to (22) and assuming the following values of the parameters [21] $\gamma_0 = 3$ eV, $\gamma_1 = 0.392$ eV, $\gamma_2 = -0.019$ eV, $\gamma_3 = 0.21$ eV, $\gamma_4 = 0.193$ eV, $\gamma_5 = 9.11$ eV, $T = 4.2$ K, $\Delta = -0.0002$ eV, $a = 24.6$ nm, $C = 67.3$ nm, $\gamma'_0 = 10^{-3}$ eV/K, $\gamma'_1 = 2 \cdot 10^{-4}$ eV/K, $\gamma'_2 = -3 \cdot 10^{-4}$ eV/K, $\gamma'_3 = -2 \cdot 10^{-3}$ eV/K, $\gamma'_4 = 2.1 \cdot 10^{-3}$ eV/K, $\gamma'_5 = 10^{-6}$ eV/K, $\Delta' = -6 \cdot 10^{-6}$ eV/K, $\theta_D = 300$ K, we have calculated the normalised HC of QWs, QWWs, QDs and MSQ of graphite as functions of doping, film thickness and the magnetic field for various temperatures. The results are shown in Figs. 1 to 8. The circles show the experimental results [21]. From the above discussions and the figures the following features follow:

1. From Fig. 1 it appears that the HC increases with increasing electron concentration per unit area in QWs of graphite in steps which reflect the dependence of the density of states function under size quantization. Fig. 2 illustrates that the HC decreases with increasing film thickness also in a step-like fashion. The steps are not perfect due to the presence of finite temperature. The temperature enhances the value of the HC in the whole ranges of variables considered in the figures. From Fig. 1, the influence of the size quantization is immediately apparent. The HC has become strongly dependent on the thickness of the ultrathin films in contrast with the HC of bulk specimens of graphite.

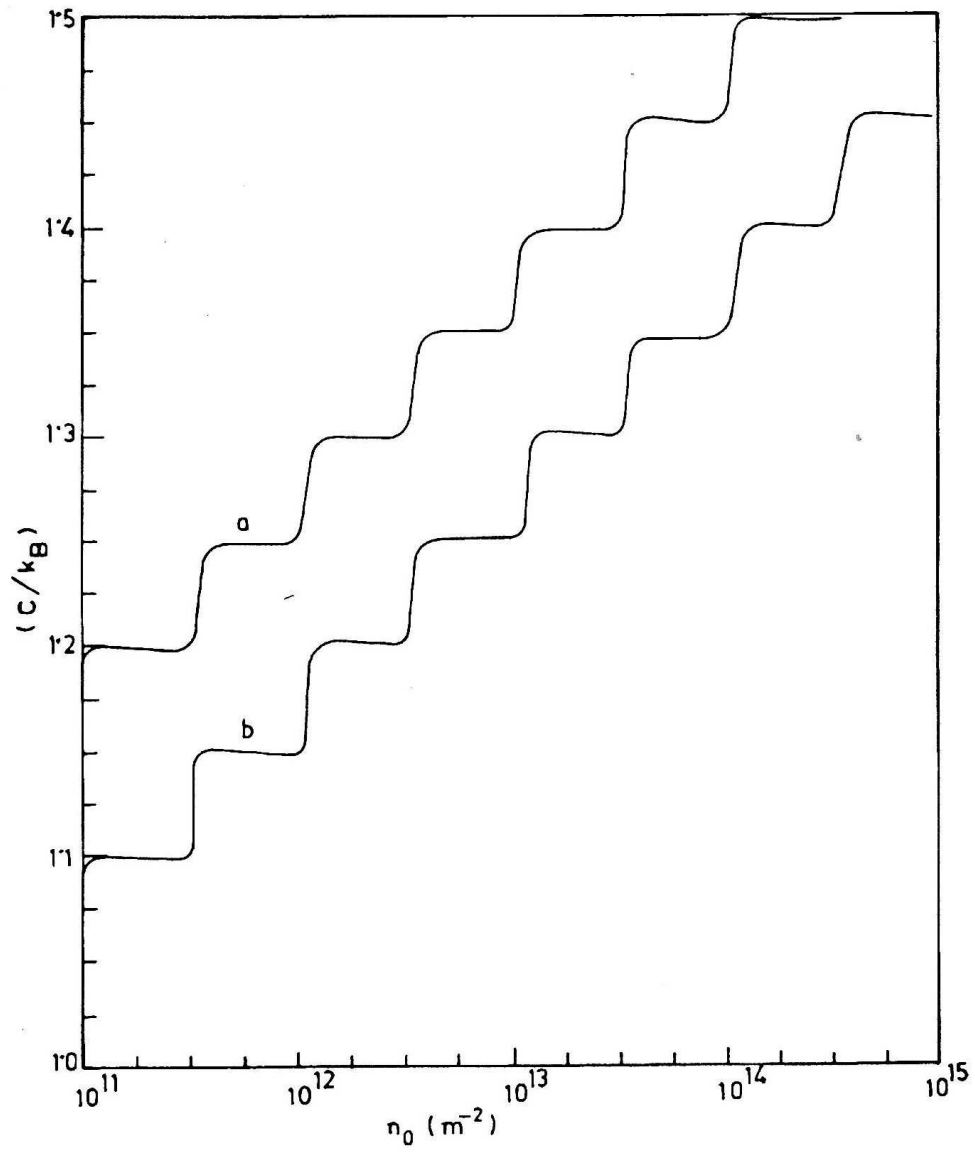


Fig. 1. Plot of the normalized HC in QWs of graphite versus surface concentration of electrons at a) 10 K and b) 4.2 K ($d_z=40$ nm).

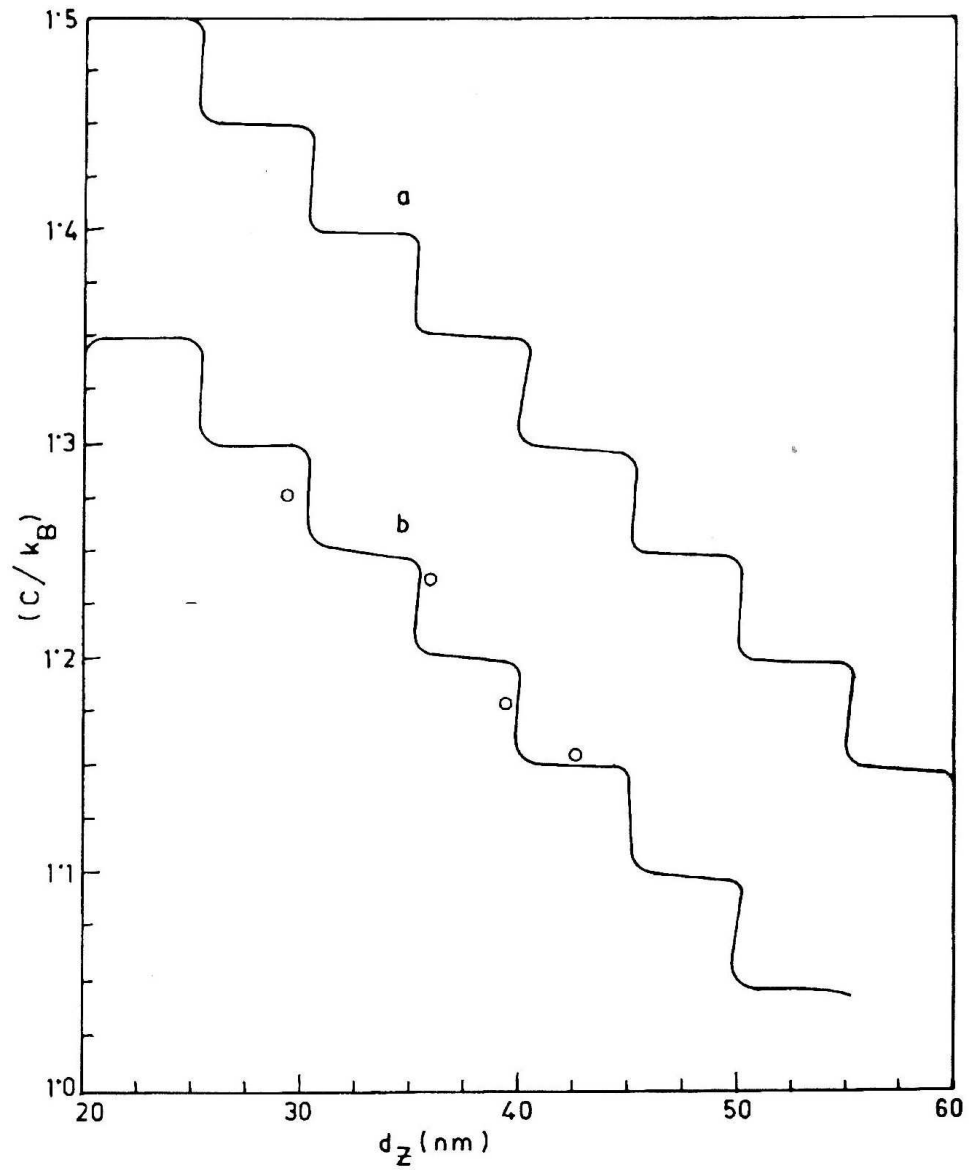


Fig. 2. Plot of the normalized HC in QWs of graphite versus film thickness d_z at a) 10 K and b) 4.2 K ($n_o=10^{14} \text{ m}^{-2}$).

2. From Fig. 3, it appears that the HC in QWWs of graphite increases with increasing electron concentration per unit length in sharp steps. From Fig. 4, it appears that the HC in QWWs of graphite decreases continuously in the electric quantum limit with increasing film thickness. Due to the 1D carrier motion, the value of the Fermi energy is greater as compared with the 2D motion. As a consequence, the value of the HC is enhanced.

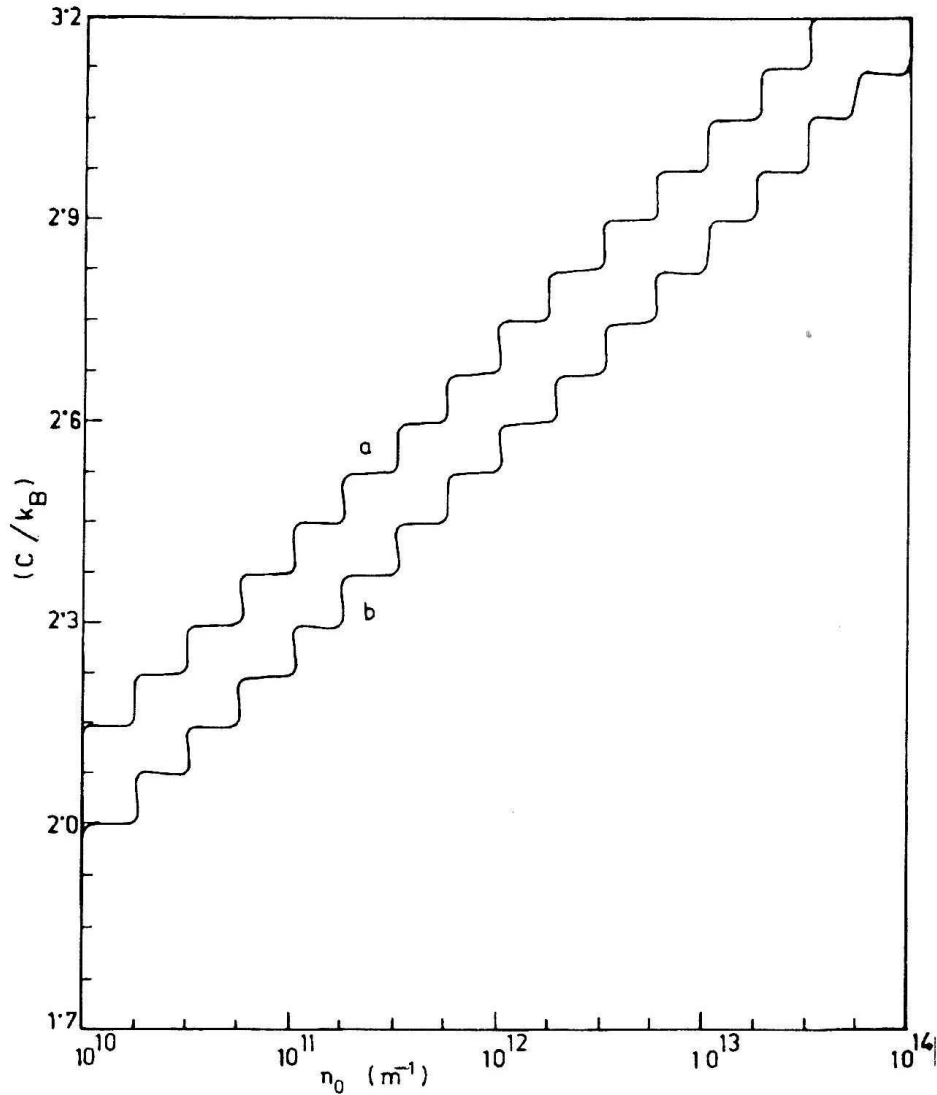


Fig. 3. Plot of the normalized HC in QWWs of graphite versus linear concentration of electrons n_0 at a) 10 K and b) 4.2 K ($d_y = d_z = 40$ nm).

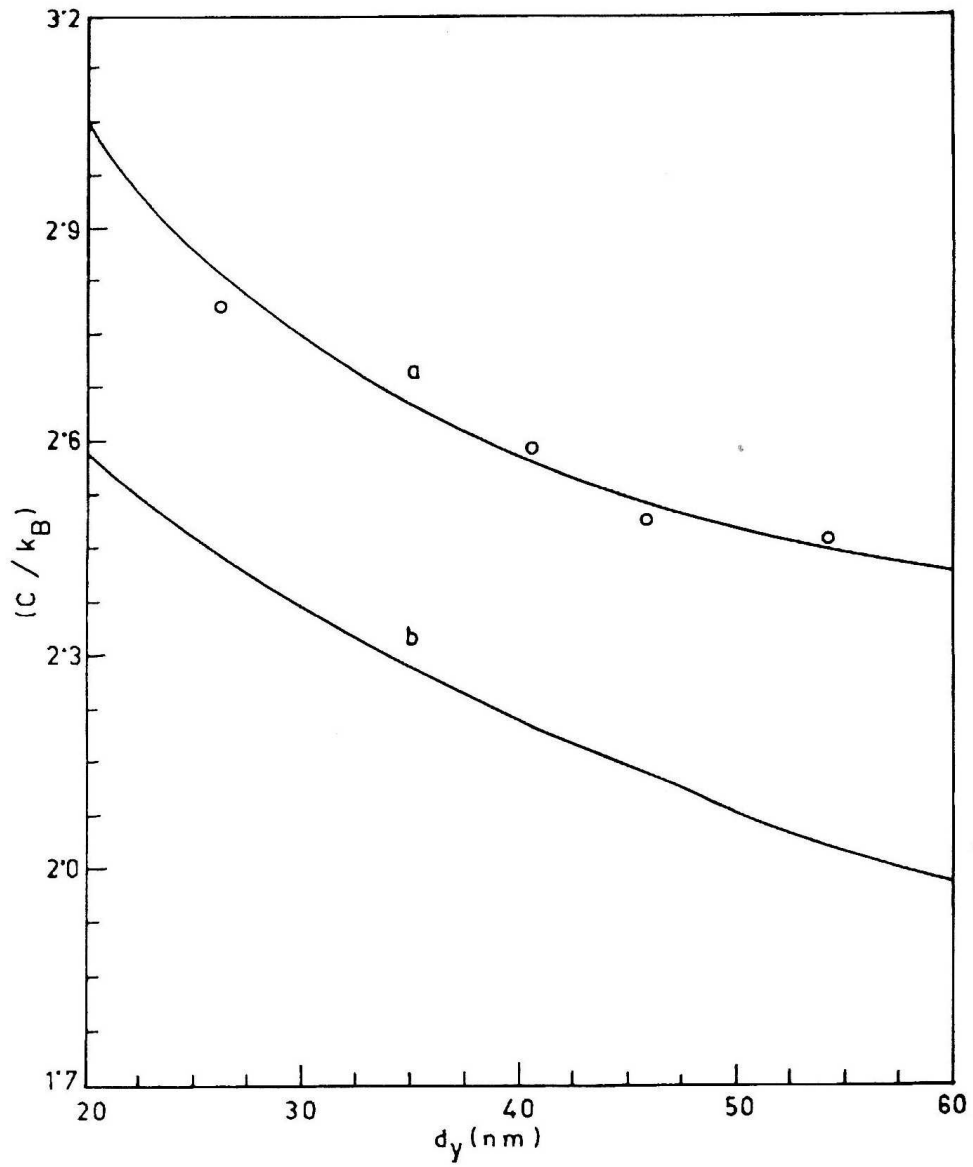


Fig. 4. Plot of the normalized HC in QWWs of graphite at the electric quantum limit ($n = t = 1$) versus film thickness d_y at a) 10 K and b) 4.2 K ($d_x = 40$ nm and $n_o = 10^{11} \text{ m}^{-1}$).

From Fig. 5, it appears that the HC decreases with increasing film thickness in QDs of graphite in the step-like fashion. From Fig. 6, it appears that the HC increases with increasing electron concentration in a monotonous manner in the electric quantum limit in QDs of graphite. It may be noted that in QDs, the 3D quantization leads to the discrete energy levels somewhat like atomic energy levels. That produces very large effects. Under such quantization, there remain no free electron states and, consequently, the crossing of the Fermi levels by the size quantized subbands has a much greater effect on the redistribution of the electrons as compared to that found for the 1D quantization. It is basically this effect that results in the enhancement of the HC under 3D quantization as found in QDs of graphite.

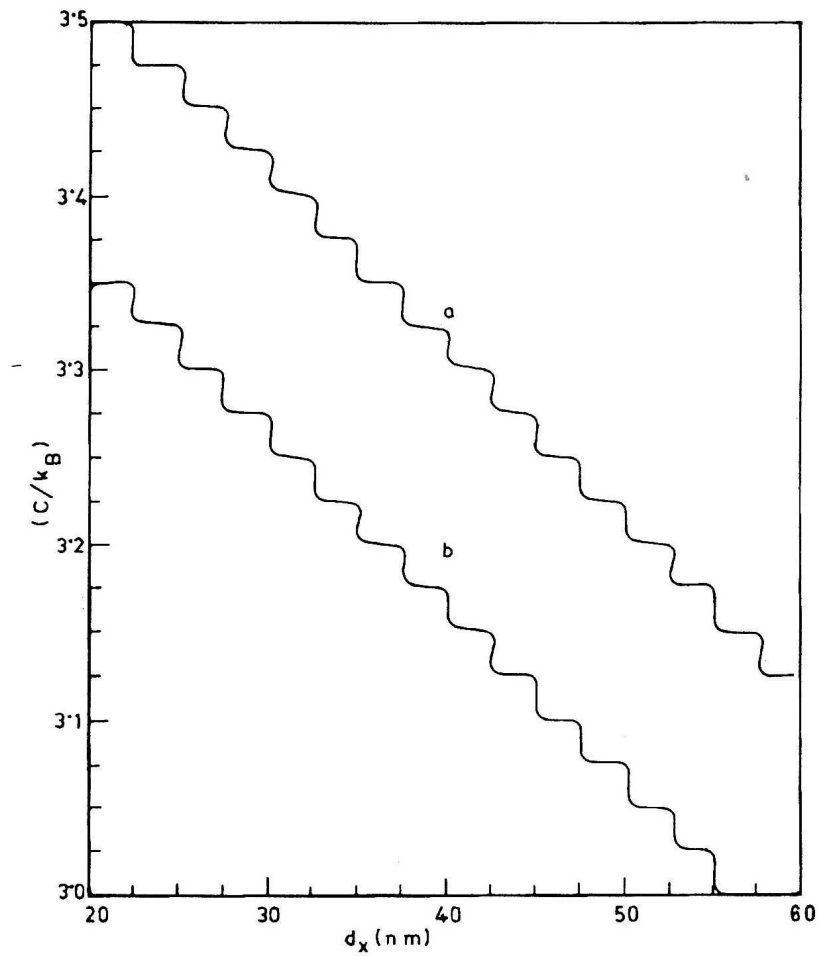


Fig. 5. Plot of the normalized HC in QDs of graphite versus film thickness d_x at a) 10 K and b) 4.2 K ($d_y = d_z = 40$ nm and $n_0 = 10^{19}$ m $^{-3}$).

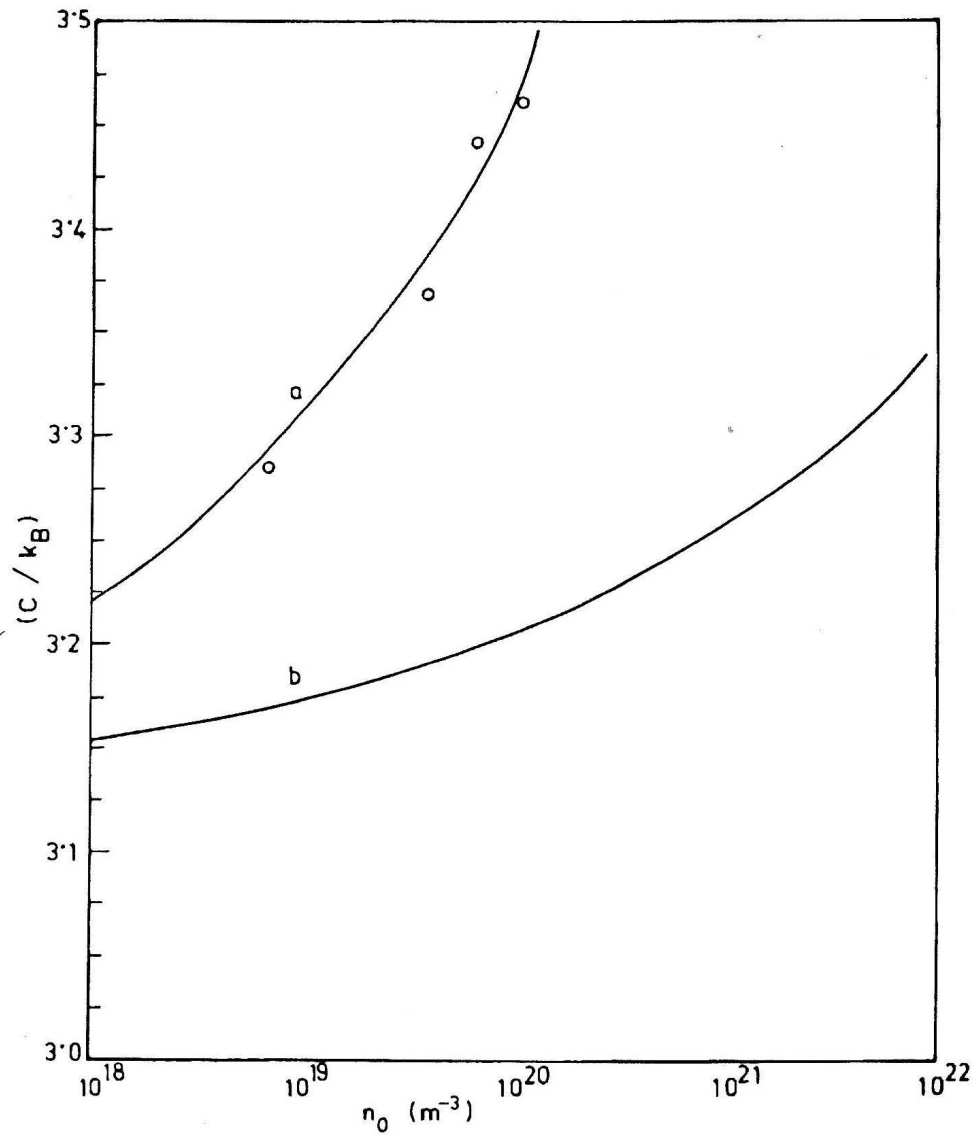


Fig. 6. Plot of the normalized HC in QDs of graphite versus n_0 at the electric quantum limit ($n = t = w = 1$) at a) 10 K and b) 4.2 K ($d_x = d_y = d_z = 40$ nm). The circles show the experimental results.

From Fig. 7, it appears that HC in magneto-sized graphite decreases in an oscillatory way with the magnetic field. The HC also increases with increasing electron concentration per unit area for the present case as shown in Fig. 8. This is another type of 3D quantization which can be produced in graphite.

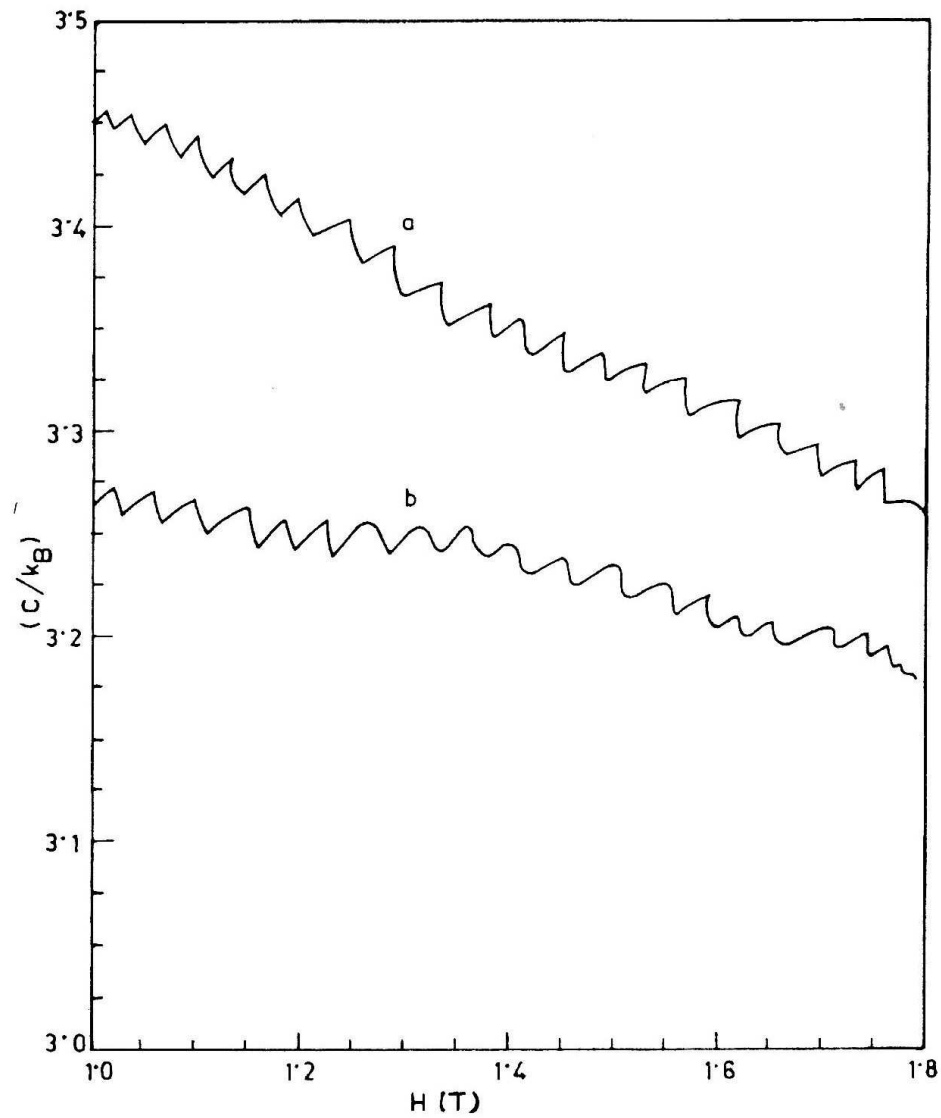


Fig. 7. Plot of the normalized HC in magneto-sized graphite versus magnetic field B at a) 10 K and b) 4.2 K ($n_o = 10^{14} \text{ m}^{-2}$, $d_z = 40 \text{ nm}$).

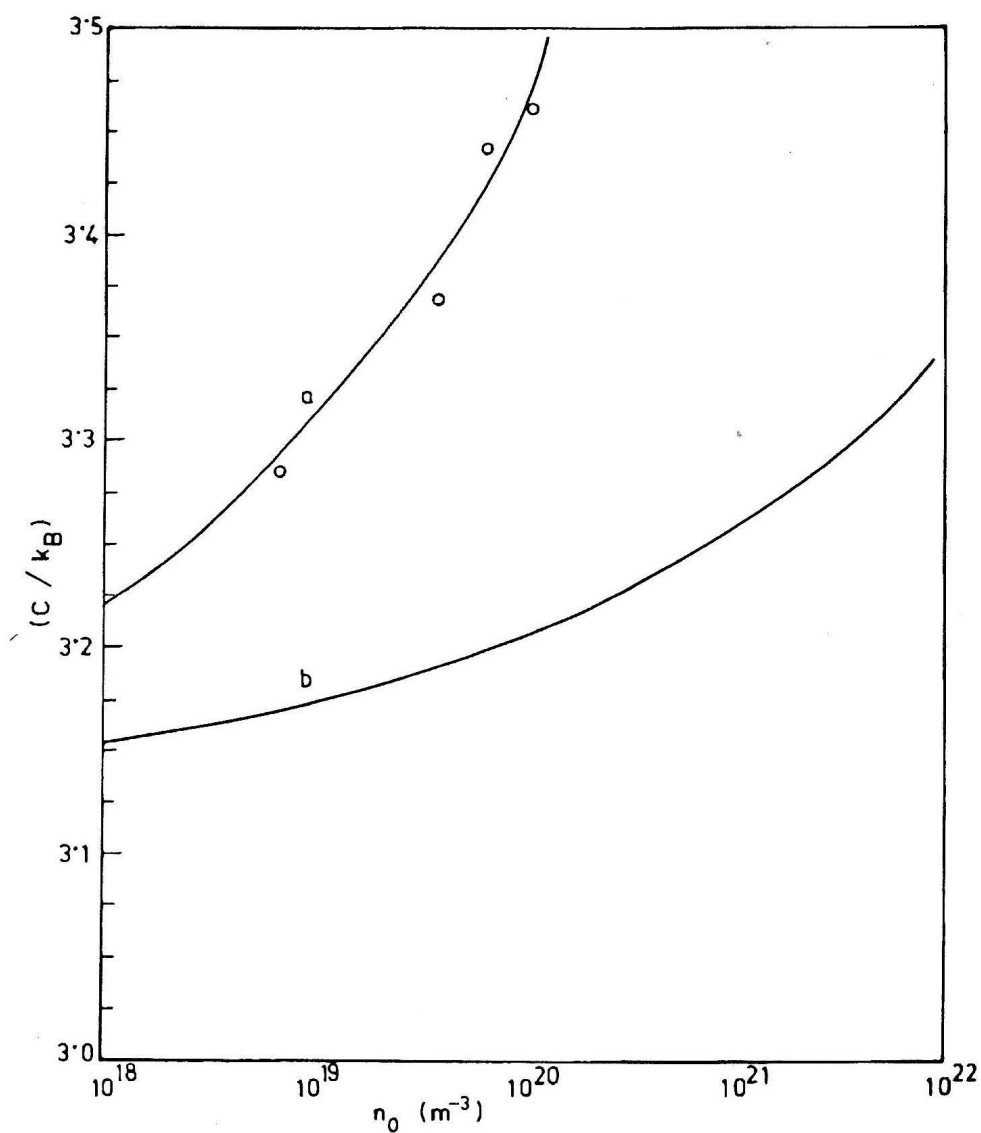


Fig. 8. Plot of the normalized HC in magneto-sized graphite versus surface concentration of electrons n_0 at a) 10 K and b) 4.2 K ($B=1$ T, $d_z=40$ nm).

In conclusion, it may be noted that the basic purpose of the present work is not solely to investigate the HC in graphite but also to formulate the appropriate density of states function since the different thermal properties of quantum confined graphite are based on the density of states function in such microstructures.

References

- 1) J. Cibert, P. M. Petroff, G. J. Dolan, S. J. Pearson, A. C. Gossard and J. H. English, *Appl. Phys. Lett.* **49** (1986) 1275;
- 2) J. M. Gaines, P. M. Petroff, H. Kroemer, R. J. Siemes, R. S. Geels and J. H. English, *J. Vac. Sci. Tech.* **6B** (1988) 824;
- 3) T. Fukui and H. Saito, *Appl. Phys. Lett.* **50** (1987) 824;
- 4) T. Ando, A. H. Fowler and F. Stern, *Rev. Mod. Phys.* **59** (1982) 437;
- 5) H. Sakaki, *Jap. J. Appl. Phys.* **19** (1980) 94;
- 6) P. M. Petroff, A. C. Gossard, R. A. Logan and W. Weigmann, *Appl. Phys. Lett.* **41** (1982) 635;
- 7) K. P. Ghatak, K. K. Ghosh, H. M. Mukherjee and A. N. Chakravarti, *Phys. Stat. Sol. (b)* **110** (1982) 323;
- 8) B. Mitra, A. Ghoshal and K. P. Ghatak, *Nouvo Cimento D* **12** (1990) 891;
- 9) K. P. Ghatak and M. Mondal, *J. Appl. Phys.* **69** (1991) 1666;
- 10) K. P. Ghatak and S. N. Biswas, *Low Temp. Phys.* **78** (1990) 219;
- 11) E. S. R. Gopal, *Specific Heats at Low Temperatures*, Plenum press, New York, 1966 and the references cited therein; B. A. Aronzon and E. Z. Meilikhov, *Sov. Phys. Semicond.* **13** (1979) 568;
- 12) M. Mondal and K. P. Ghatak, *Acta. Phys. Polon.* **A66** (1984) 539;
- 13) A. N. Chakravarti, K. P. Ghatak, S. Ghosh and A.K. Chowdhury, *Phys. Stat. Sol. (b)* **109** (1982) 706;
- 14) K. P. Ghatak, A. Ghoshal, S. Bhattacharyya and M. Mondal, *SPIE* **1313** (1990) 225;
- 15) C. C. Tien and J. H. Lienhard, *Statistical Thermodynamics*, Holt, Rienhart and Winston, Inc., New York, 1971;
- 16) A. A. Abrikosov, *Introduction to the Theory of Normal Metals*, Supplement **12** of the series of Solid State Physics, Advances in Research and Applications, Editors H. Ehrenreich, F. Seitz and D. Turnbull, p. 32, 1972;
- 17) H. Ushio, T. Dau and Y. Uumura, *J. Phys. Soc. Japan* **33** (1972) 1551;
- 18) J. S. Blakemore, *Semiconductor Statistics*, Dover Publications, New York, 1987;
- 19) K. P. Ghatak and B. Mitra, *Int. J. Electronics* **72** (1992) 541;
- 20) M. Abramowitz and I. A. Stegun, *Handbook of Mathematical Functions*, Dover, New York, 1965;
- 21) L. Bandt and I. M. Tsidilkovskii, *The Electronic Properties of Graphite*, Nauka Press, Moskva, 1991.

UTJECAJ KVANTNOG ZASUŽNJENJA NA TOPLINSKI KAPACITET
GRAFITA

KAMAKHYA P. GHATAK i S. N. BISWAS

*Department of Electronic Science, University of Calcutta, 92 Acharya Prafulla
Chandra Road, University College of Science and Technology, Calcutta-700009,
India*

and

*Department of Electronics and Telecommunication Engineering, Bengal
Engineering College, Shibpur, Howrah - 711103, West Bengal, India*

UDK 538.95

PACS 65.40.Em

Pokušava se objasniti toplinski kapacitet grafita u kojem postoji kvantno zasušnjenje u jednoj, dvije ili tri dimenzije, tj. u kvantnim jamama, kvantnim žicama, kvantnim točkama, te sistemima s magnetski-ograničenom kvantizacijom stanja vrpce zaključivanjem o odgovarajućem obliku funkcije gustoće stanja. Pri tome se uzimaju u obzir razni oblici anizotropije konstanti energetske vrpce. Nađeno je da toplinski kapacitet titra kao funkcija debljine sloja, magnetskog polja i dopiranja. Toplinski kapacitet je najveći u kvantnim točkama, a najmanji u kvantnim jamama. Teorijska analiza u skladu je s rezultatima mjerenja.